Quantum Chemical Studies of Some Rhodanine Azosulpha Drugs as Corrosion Inhibitors for Mild Steel in Acidic Medium

ARTICLE *in* INTERNATIONAL JOURNAL OF QUANTUM CHEMISTRY · APRIL 2009

Impact Factor: 1.43 · DOI: 10.1002/qua.22249

5 AUTHORS, INCLUDING:

Eno Ebenso
North West University South Africa
192 PUBLICATIONS **3,223** CITATIONS
SEE PROFILE

Taner Arslan
Eskisehir Osmangazi University
37 PUBLICATIONS **444** CITATIONS
SEE PROFILE

Fatma Kandemirli
Kastamonu Üniversitesi
86 PUBLICATIONS **1,192** CITATIONS
SEE PROFILE

Necmettin Caner
Eskisehir Osmangazi University
22 PUBLICATIONS **123** CITATIONS
SEE PROFILE

Quantum Chemical Studies of Some Rhodanine Azosulpha Drugs as Corrosion Inhibitors for Mild Steel in Acidic Medium

ENO E. EBENSO,[1] TANER ARSLAN,[2] FATMA KANDEMIRLI,[3] NECMETTIN CANER,[2] IAN LOVE[1]

[1]*Department of Chemistry, North West University (MafiKeng Campus), Private Bag ×2046, Mmabatho 2735, South Africa*

[2]*Department of Chemistry, Eskisehir Osmangazi University, 26480 Eskisehir, Turkey*

[3]*Department of Chemistry, Kocaeli University, 41380 Izmit, Turkey*

[4]*Department of Chemistry and Chemical Technology, National University of Lesotho, P.O. Roma 180, Lesotho, Southern Africa*

Received 18 November 2008; accepted 9 March 2009
Published online 10 August 2009 in Wiley InterScience (www.interscience.wiley.com).
DOI 10.1002/qua.22249

ABSTRACT: The density functional theory (DFT) at the B3LYP/6-31G (d,p) and B3LYP/6-311G(d,p) basis set levels and ab initio calculations using the HF/6-31G (d,p) and HF/6-311G(d,p) methods were performed on four rhodanine azosulpha drugs (namely 5-sulfadiazineazo-3-phenyl-2-thioxo-4-thiazolidinone, 5- sulfamethazineazo-3-phenyl-2-thioxo-4-thiazolidinone, 5-sulfadimethoxineazo-3-phenyl-2-thioxo- 4-thiazolidinone, and 5-sulfamethoxazoleazo-3-phenyl-2-thioxo-4-thiazolidinone) used as corrosion inhibitors for mild steel in acidic medium to determine the relationship between the molecular structure of the rhodanine azosulpha drugs and inhibition efficiency(%IE). The quantum chemical parameters/descriptors, namely, E_{HOMO} (highest occupied molecular orbital energy), E_{LUMO} (lowest unoccupied molecular orbital energy), the energy difference (ΔE) between E_{HOMO} and E_{LUMO}, dipole moment (μ), electron affinity (**A**), ionization potential (**I**), the absolute electronegativity (**X**), absolute hardness (η), softness (σ), polarizability (α), the Mulliken charges, and the fraction of electrons (Δ**N**) transfer from inhibitors to iron, were calculated and correlated with the experimental %IE. Quantitative structure activity relationship (QSAR) approach has

Correspondence to: E. E. Ebenso; e-mail: eno_ebenso@yahoo.com

Contract grant sponsor: Scientific and Technological Research Council of Turkey (Visiting Scientist Supporting Program).

been used, and a composite index of some quantum chemical parameters/descriptors was performed to characterize the inhibition performance of the studied molecules. The results showed that the inhibition efficiency (%IE) of the rhodanine azo sulfa drugs studied was closely related to some of the quantum chemical parameters/descriptors but with varying degrees of correlation coefficient (R^2). The %IE also increased with the increase in E_{HOMO} and decrease in $E_{HOMO}-E_{LUMO}$; and the areas containing N atoms are the most possible sites for bonding to the metal iron surface by donating electrons to the metal. The HOMO orbitals consist of 61.73–63.04% double bonded S atom (7(S)), and most of the rest are concentrated on the rhodanine group; so, the rhodanine molecule plays an important role in bonding of sulfa drugs with metal atom in the corrosion process. The calculated/estimated %IE of the compounds studied was found to be close to the experimental %IE. Int J Quantum Chem 110: 1003–1018, 2010

Key words: rhodanine azosulpha drugs; density functional theory (DFT); ab initio calculations; corrosion inhibitors

Introduction

The use of corrosion inhibitors is one of the most effective means of protecting metal and alloy surfaces against corrosion in acid and basic environments [1]. Generally, inhibitor molecules may physically or chemically adsorb on a corroding metal surface. In any case, adsorption is generally over the metal surface forming an adsorption layer that functions as a barrier protecting the metal from corrosion [2, 3]. It has been commonly recognized that an organic inhibitor usually promotes formation of a chelate on a metal surface, by transferring electrons from the organic compounds to the metal and forming a coordinate covalent bond during the chemical adsorption [4]. In this way, the metal acts as an electrophile; and the nucleophile centers of inhibitor molecule are normally heteroatoms with free electron pairs that are readily available for sharing, to form a bond [5]. The power of the inhibition depends on the molecular structure of the inhibitor. Organic compounds, containing functional electronegative groups and π-electron in triple or conjugated double bonds, are usually good inhibitors. Heteroatoms, such as sulfur, phosphorus, nitrogen, and oxygen, together with aromatic rings in their structure are the major adsorption centers. The planarity and the lone electron pairs in the heteroatoms are important features that determine the adsorption of molecules on the metallic surface [6].

Theoretical chemistry has been used recently to explain the mechanism of corrosion inhibition, such as quantum chemical calculations that have been proved to be a very powerful tool for studying the mechanism [7–14]. Quantum chemical studies have been successfully performed to link the corrosion inhibition efficiency with molecular orbitals (MO) energy levels for some kinds of organic compounds, for example, amides [5, 15], of amino acids and hydroxy carboxylic acids [16] pyridine–pyrazole compound [17], sulfonamides [18] to mention but a few. Abdallah [19] has studied the corrosion inhibition efficiency of four rhodanine azosulpha drugs (5-sulfadiazineazo-3-phenyl-2-thioxo-4- thiazolidinone, 5-sulfamethazineazo-3-phenyl-2-thioxo-4-thiazolidinone,5-sulfadimethoxineazo-3- phenyl-2-thioxo-4-thiazolidinone, and 5-sulfamethoxazoleazo-3-phenyl-2-thioxo-4-thiazolidinone) on 314 stainless steel in 1.0 M HCl solutions using both weight loss and potentiostatic polarization techniques and found that the compounds reduced the corrosion of mild steel, but no study using theoretical methods has been employed to investigate the correlation between the inhibition efficiency and molecular structure of the sulfa drugs compounds yet.

Therefore, the objective of this study is to present a theoretical study on the electronic and molecular structures of 5-sulfadiazineazo-3-phenyl-2-thioxo-4-thiazolidinone (npyrm), 5-sulfa methazineazo-3-phenyl-2-thioxo-4-thiazolidinone (ndimepyrm), 5-sulfadimethoxineazo-3-phenyl-2-thioxo-4-thiazolidinone (ndimetoxpyr), and 5-sulfamethoxazoleazo-3-phenyl-2-thioxo-4-thiazolidinone (nisox) compounds used as inhibitor and to determine the relationship between some quantum chemical descriptors/parameters obtained from the molecular structure of the compounds and inhibition efficiency studied using the ab initio

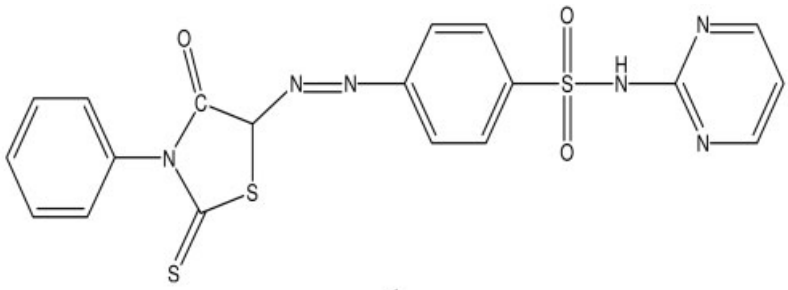

1

5-sulphadiazineazo-3-phenyl-2-thioxo-4-thiazolidinone (npyrm)

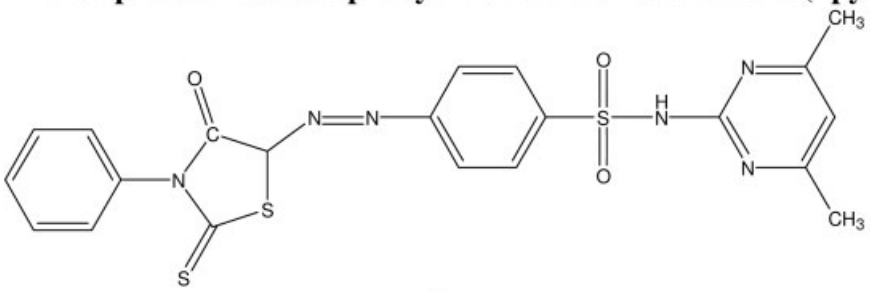

2

5-sulphamethazineazo-3-phenyl-2-thioxo-4-thiazolidinone (ndimepyrm)

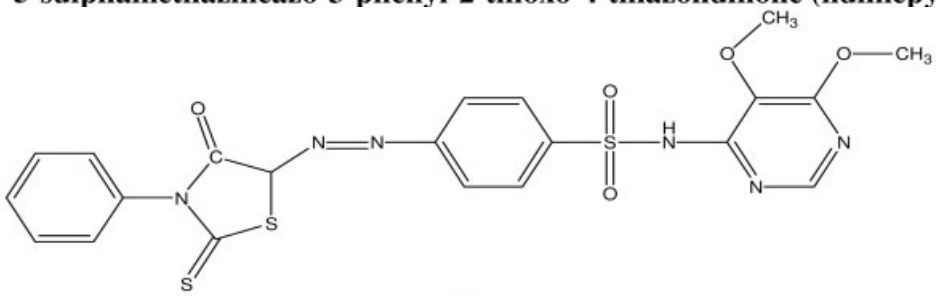

3

5-sulphadimethoxineazo-3-phenyl-2-thioxo-4-thiazolidinone (ndimetoxpyr)

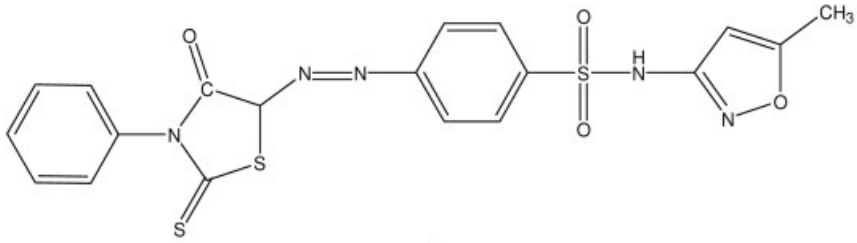

4

5-sulphamethoxazoleazo-3-phenyl-2-thioxo-4-thiazolidinone (nisox)

methods of HF/6-31G (d,p) and HF/6-311G(d,p) and density functional theory (DFT) at the B3LYP/6-31G (d,p) and B3LYP/6-311G(d,p) basis set levels. Our aim is to find good theoretical parameters to characterize the inhibition property of the inhibitors, to establish the correlation between the inhibition efficiency and the electronic properties of the studied molecules using different methods and basis sets. The structures of the rhodanine azosulpha drugs used in this study are given above;

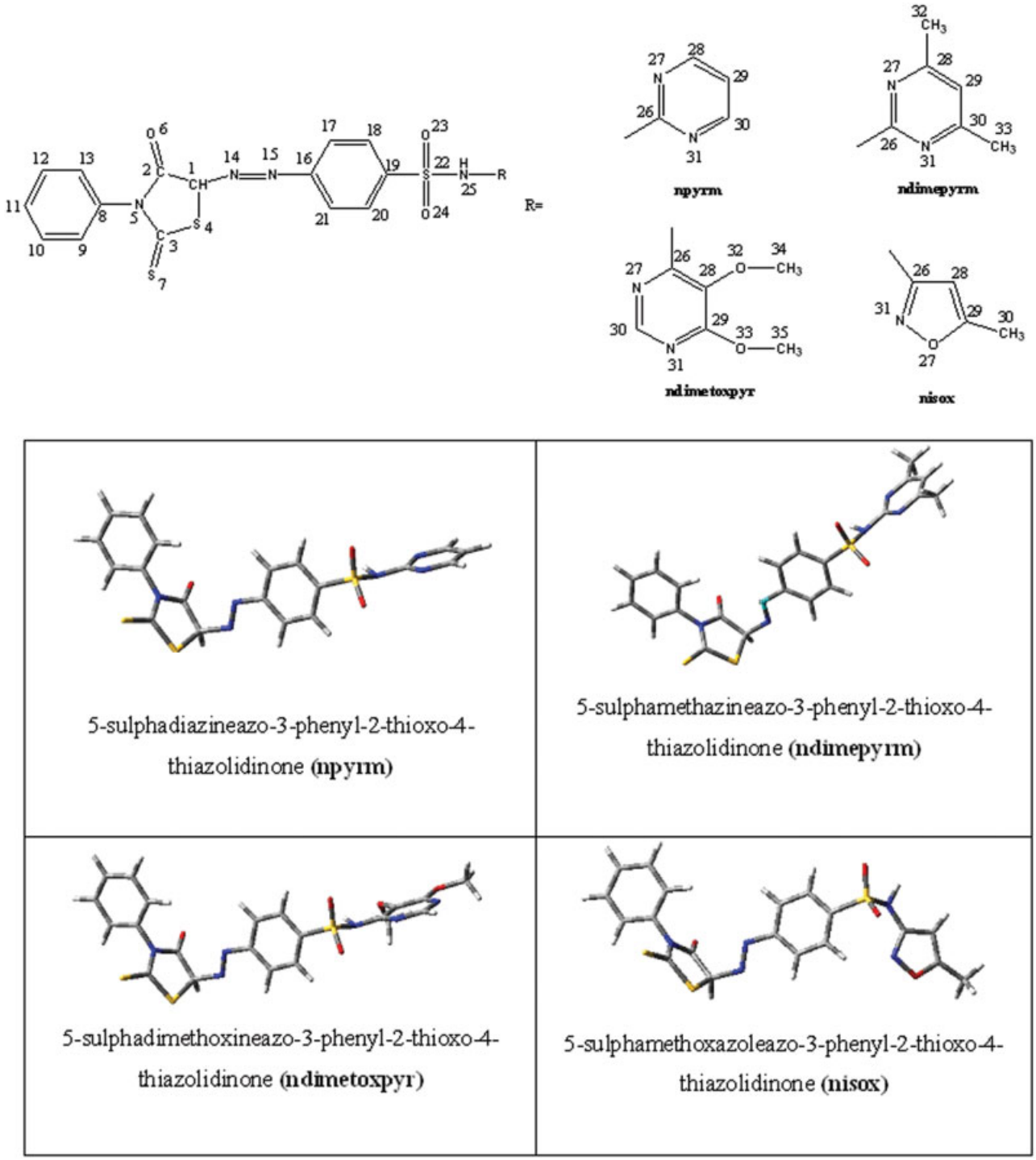

FIGURE 1. The optimized geometries and the numbering scheme of the four rhodanine azo sulfa drugs studied. [Color figure can be viewed in the online issue, which is available at www.interscience.wiley.com.]

TABLE I

Calculated energies (in a.u.) levels of the HOMO, LUMO, $\Delta E_{HOMO-LUMO}$ (ΔE) and measured average inhibition efficiencies (%IE) for the series of studied molecules.

Molecules		npyrm	ndimepyrm	ndimetoxpyr	nisox
HF/6-31G(d,p)	E_{HOMO}	−0.3417	−0.3411	−0.3423	−0.3359
	E_{LUMO}	0.0392	0.0408	0.0382	0.0353
	$\Delta E_{HOMO-LUMO}$	−0.3809	−0.3819	−0.3805	−0.3712
HF/6-311G(d,p)	E_{HOMO}	−0.3457	−0.3451	−0.3462	−0.3430
	E_{LUMO}	0.0333	0.0349	0.0326	0.0392
	$\Delta E_{HOMO-LUMO}$	−0.3790	−0.3800	−0.3787	−0.3822
B3LYP/6-31G(d,p)	E_{HOMO}	−0.2348	−0.2339	−0.2351	−0.2327
	E_{LUMO}	−0.1096	−0.1076	−0.1087	−0.1055
	$\Delta E_{HOMO-LUMO}$	−0.1253	−0.1263	−0.1264	−0.1273
B3LYP/6-311G(d,p)	E_{HOMO}	−0.2427	−0.2419	−0.2428	−0.2390
	E_{LUMO}	−0.1170	−0.1153	−0.1165	−0.1096
	$\Delta E_{HOMO-LUMO}$	−0.1257	−0.1266	−0.1263	−0.1293
%IE Average		81.10	87.73	93.72	66.52

Calculation Methods

The molecular sketches of the rhodanine azosulpha drugs were drawn using the GaussView 3.0. All the quantum chemical calculations were performed with complete geometry optimizations using standard Gaussian-03 (Review B.05) software package [20]. Geometry optimizations and quantum chemical calculations were performed using ab initio calculations and the density functional theory (DFT). Ab initio calculations were carried out using the Hartree–Fock (HF) method. The Becke's three-parameter hybrid functional [21–23] was combined with the Lee, Yang, and Parr (LYP) correlation functional [24] and denoted as B3LYP and [22] was employed in the DFT calculations using the 6-31G(d,p) and 6-311G(d,p) basis set levels. The same basis set levels were also used for the HF method.

Recently, the density functional theory (DFT) has been used to analyze the characteristics of the inhibitor/surface mechanism and to describe the structural nature of the inhibitor on the corrosion process [15, 25–37]. Furthermore, DFT is considered a very useful technique to probe the inhibitor/surface interaction as well as to analyze the experimental data. The density functional theory (DFT) [38] has been found to be successful in providing insights into the chemical reactivity and selectivity, in terms of global parameters such as electronegativity (χ) [39], hardness (η) [40] and softness (S)[40], and local ones such as the Fukui function ($f(\vec{\mathbf{r}})$) [41] and local softness ($s(\vec{\mathbf{r}})$) [42]. Thus, for an N-electron system with total electronic energy (E) and an external potential ($\upsilon(\vec{\mathbf{r}})$); chemical potential ($\mu$) [39] known as the negative of electronegativity (χ), has been defined as the first derivative of the E with respect to N at $\upsilon(\vec{\mathbf{r}})$ [43].

$$\chi = -\mu = -\left(\frac{\partial E}{\partial N}\right)_{v(r)} \tag{1}$$

Hardness (η) has been defined within the DFT as the second derivative of the E with respect to N at $\upsilon(\vec{\mathbf{r}})$ [44].

$$\eta = \frac{1}{2}\left(\frac{\partial^2 E}{\partial N^2}\right)_{v(r)^*} \tag{2}$$

The number of transferred electrons (ΔN) was also calculated depending on the quantum chemical method [45, 46] by using the equation below;

$$\Delta N = \frac{\chi_{Fe} - \chi_{\text{inh}}}{[2(\eta_{Fe} + \eta_{\text{inh}})]} \tag{3}$$

where χ_{Fe} and χ_{inh} denote the absolute electronegativity of iron and the inhibitor molecule, respectively; η_{Fe} and η_{inh} denote the absolute hardness of iron and the inhibitor molecule, respectively. I and A are related in turn to E_{HOMO} and E_{LUMO} using the equations below;

$$I = -E_{\text{HOMO}} \tag{4}$$

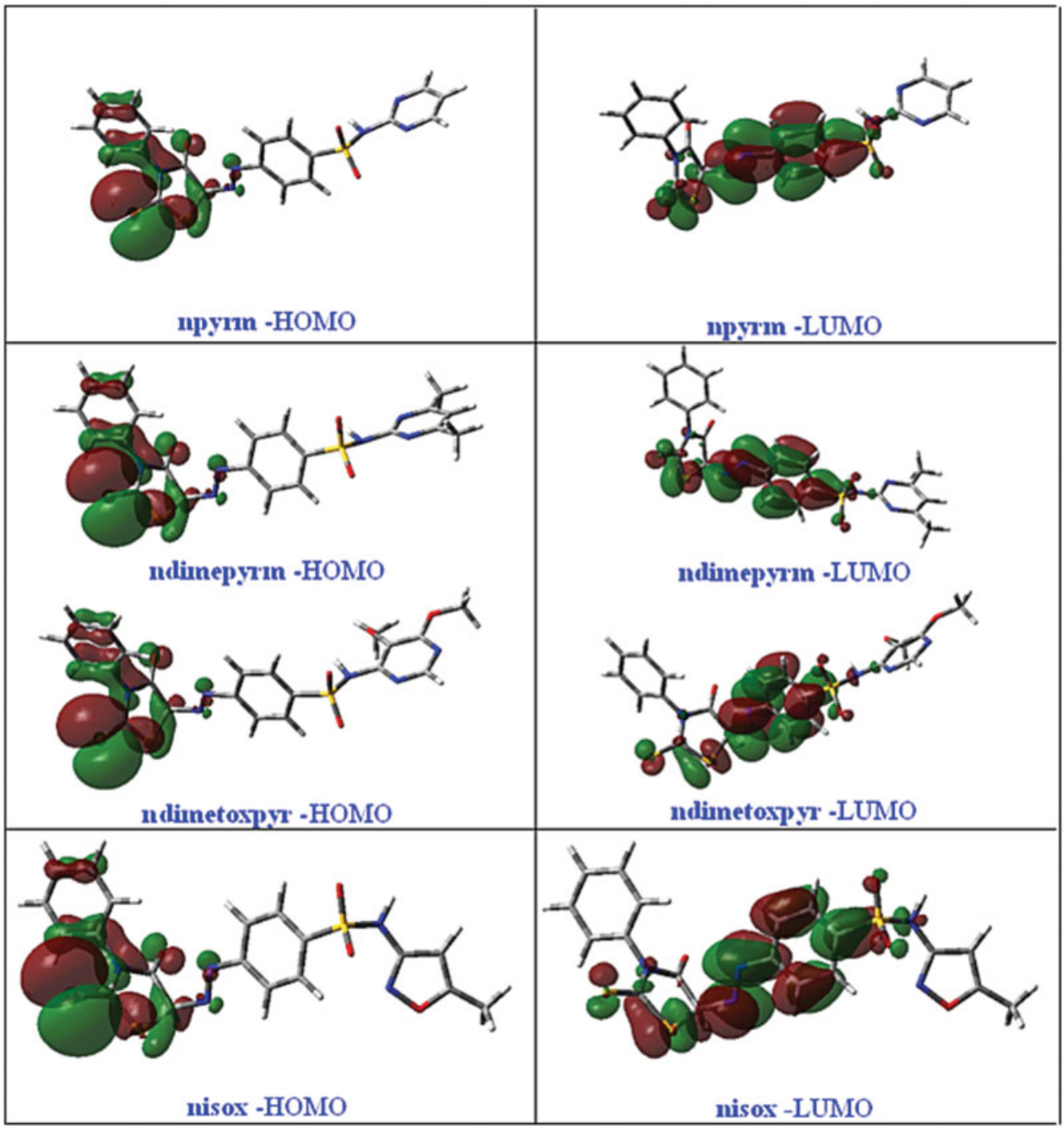

FIGURE 2. HOMO and LUMO orbital contributions of the studied molecules at B3LYP/6-31G(d,p) level. [Color figure can be viewed in the online issue, which is available at www.interscience.wiley.com.]

$$A = -E_{\mathrm{LUMO}} \tag{5}$$

These quantities are related to electron affinity (A) and ionization potential (I) using the equations below;

$$\chi = \frac{I + A}{2}, \chi = -\frac{E_{\mathrm{LUMO}} + E_{\mathrm{HOMO}}}{2} \tag{6}$$

$$\eta = \frac{I - A}{2}, \eta = \left(\frac{E_{\mathrm{LUMO}} - E_{\mathrm{HOMO}}}{2}\right) \tag{7}$$

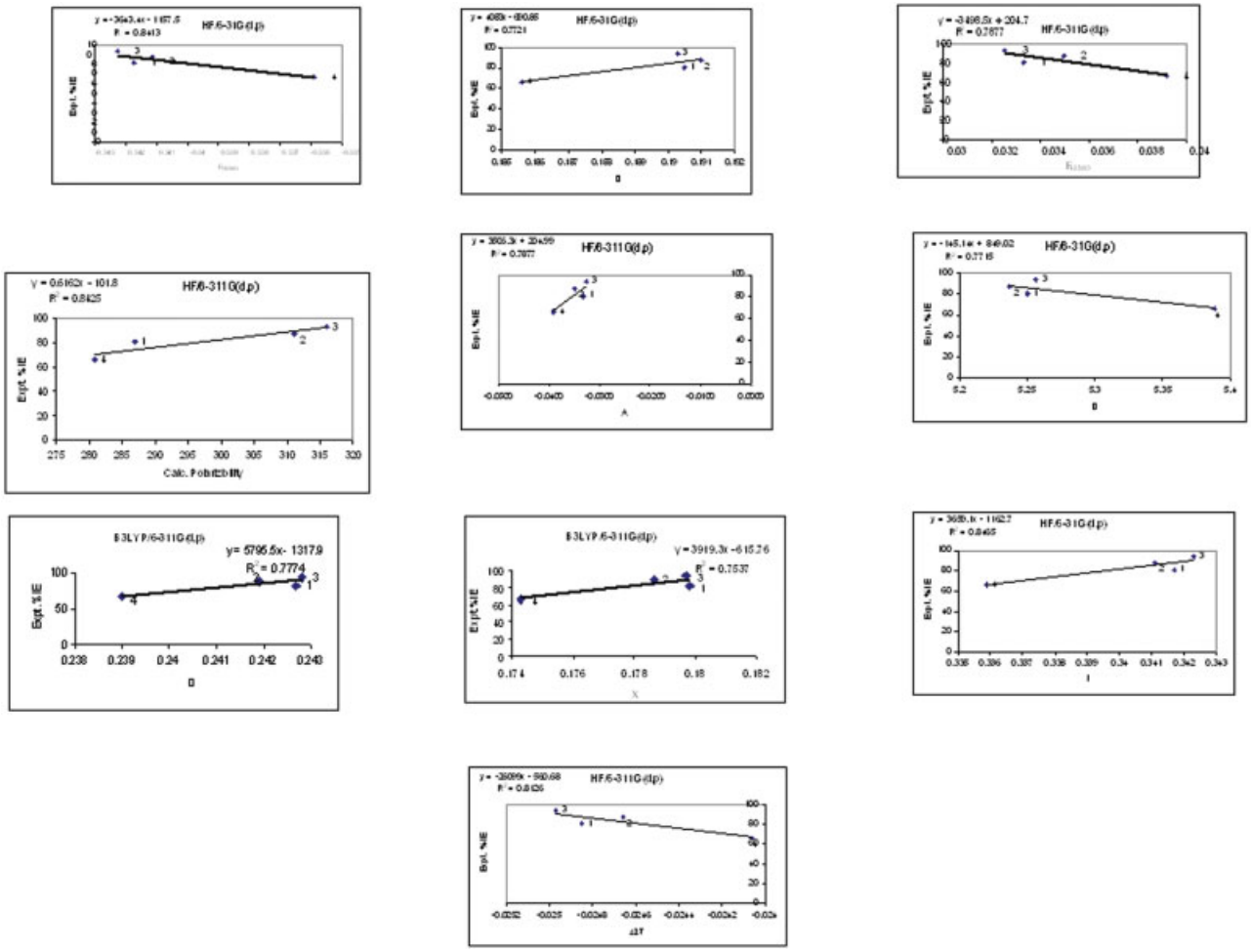

FIGURE 3. Correlations between experimental %IE and different quantum chemical parameters for the four rhodanine azo sulfa drugs studied using the different methods (1, npyrm; 2, ndimepyrm; 3, ndimetoxpyr; 4, nisox). [Color figure can be viewed in the online issue, which is available at www.interscience.wiley.com.]

Another way of obtaining information about the distribution of electrons is made by computing polarizability. The electric dipole polarizability, (α) value was calculated using Eq. (8) below:

$$< \alpha > = \frac{1}{3}(\alpha_{xx} + \alpha_{xx} + \alpha_{zz}) \qquad (8)$$

Results and Discussion

The optimized geometry of the four rhodanine azosulpha drugs obtained with B3LYP/6-31G(d,p) and the scheme showing the numbering of the parts of the studied molecules are shown in Figure 1.

Table I shows the calculated values of the highest occupied molecular orbital energy, E_{HOMO}, the lowest unoccupied molecular orbital energy, E_{LUMO}, and the measured average corrosion inhibition efficiency (%IE) for the four rhodanine azosulpha compounds used as inhibitors.

As seen in Table I, ndimetoxpyr has the highest experimental %IE value and lowest calculated E_{HOMO} whereas nisox has the lowest experimental %IE and the highest calculated E_{HOMO} using the HF/6-31G(d,p) and B3LYP/6-311G(d,p) levels. Abdallah [19] reported that the inhibition efficiency obtained for the rhodanine azo sulpha drugs is in the order; ndimetoxpyr > ndimepyrm > npyrm > nisox. From Table I, the results obtained from the calculated average %IE

TABLE II

HOMO atomic orbital coefficients of the studied molecules at B3LYP/6-31G(d,p) level.

		npyrm	ndimepyrm	ndimetoxpyr	nisox
3 (C)	3PY	0.1063	0.1138	0.1159	–
%Density		1.13	1.29	1.34	–
4(S)	3PZ	0.1142	−0.1073	−0.1282	0.1198
%Density		1.30	1.15	1.64	1.43
5(N)	3S	–	−0.1915	−0.1930	−0.1910
	3PX	–	–	0.1001	–
%Density		–	3.66	4.72	3.65
7(S)	2PX	–	–	–	0.1064
	2PY	−0.2359	−0.2358	−0.2181	−0.2149
	3PX	0.2036	0.1901	0.1772	−0.2790
	3PY	0.6202	0.6201	0.5738	0.5647
	3PZ	–	–	−0.2620	−0.1787
	4PX	0.1198	0.1120	0.1047	−0.1636
	4PY	0.3587	0.3585	0.3308	0.3276
	4PZ	–	–	−0.1535	−0.1011
%Density		62.47	61.73	62.08	63.04

obtained in this study show the same trend. This order reflects the important role played by the molecular size and the substituent groups of the inhibitor molecule as well as the types of functional group adsorption atom in the inhibition process [18]. According to Abdallah [19], the inhibiting effect of these compounds can be attributed to their parallel adsorption at the metal solution interface. The parallel adsorption is attributed to the presence of one or more active centers for adsorption. Chemisorption takes place by the formation of a chemical bond between the metal and the adsorbed molecule, and it involves charge sharing or charge transfer from the inhibitor molecule to the metal surface forming coordinate bond. This sequence of inhibition efficiency can be explained according to (a) nisox with a five-membered ring is less efficient compared with other compounds containing with a six-membered ring. This behavior is supported by high donation of $\prod$ -electrons present in the six-membered ring. In addition, the presence of oxygen as a second heteroatom in nisox leads to decrease in the aromatic character due to electron withdrawing effect than nitrogen atom, (b) it is known that the inhibiting effect of organic compounds increase as the basicity of compounds studied increase. The nisox is less efficient compared with the other compounds (npyrm, ndimepyrm, and ndimetoxpyr). This result is because of the presence of O-atom (−I effect), which decreases the delocalization of lone pairs of electrons on the N-atom. On the other hand, ndimetoxpyr is more efficient due to the presence of two methoxy groups which increase the delocalization of lone pair on nitrogen atom. Also the methyl groups in ndimepyrm increase moderately the localization of lone pairs on nitrogen atom.

Figure 2 shows the HOMO and LUMO orbital contributions of the studied molecules at the B3LYP/6-31G (d,p) level. Figure 3 shows some representative plots of correlations made for the correlation between the experimental %IE and some of the quantum chemical parameters/descriptors for the different methods. In this study, only the correlations that have good coefficient of correlation (R^2) were reported but those with poor correlations were discarded. Generally, better correlations were obtained using the HF method than the B3LYP method in this study.

Excellent corrosion inhibitors are usually those organic compounds which not only offer electrons to unoccupied orbitals of the metal but also accept free electrons from the metal [5, 9]. The effectiveness of an inhibitor can be related to its electronic and spatial molecular structure. Also, there are certain quantum-chemical parameters/descriptors that can be related to the interactions of metal-inhibitor, namely: the E_{HOMO}, AO coefficients of the atoms which are going to form HOMO, polarizability, charges, hardness, electronegativity, and so

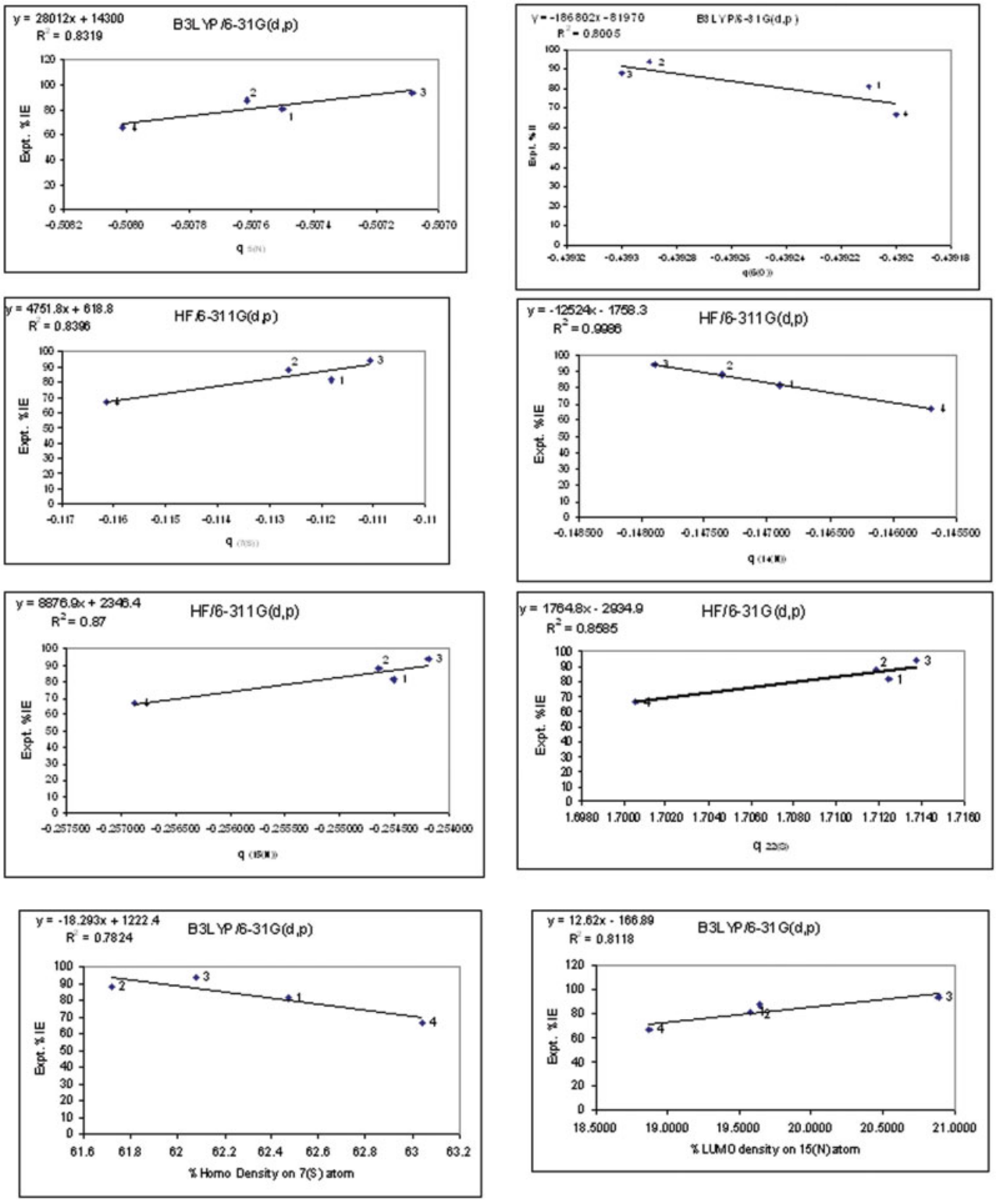

FIGURE 4. Correlations between experimental %IE and the charges/% HOMO and LUMO densities on some atoms from the four rhodanine azo sulfa drugs studied using the different methods (1, npyrm; 2, ndimepyrm; 3, ndimetoxpyr; 4, nisox). [Color figure can be viewed in the online issue, which is available at www.interscience.wiley.com.]

TABLE III

LUMO atomic orbital coefficients of the studied molecules at B3LYP/6-31G(d,p) level.

Number		npyrm	ndimepyrm	ndimetoxpyr	nisox			npyrm	ndimepyrm	ndimetoxpyr	nisox
2(C)	3S	−0.1152	−0.1148	−0.1100	0.1122		2PY	–	–	−0.1001	–
%Density		1.33	1.32	1.21	1.26	16 (C)	2PZ	−0.1423	−0.1254	−0.1036	−0.1518
							3PY	–	–	−0.1178	–
	3PX	−0.1293	−0.1321	−0.1426	−0.1140		3PZ	−0.1545	−0.1366	−0.1096	−0.1635
4(S)	3PY	–	–	0.1141	–	%Density		4.41	3.44	4.66	4.98
	3PZ	0.1130	–	–	0.1354						
%Density		2.95	1.74	3.33	3.13		2PY	–	–	0.1035	–
						17(C)	2PZ	0.1464	0.1325	0.1119	0.1613
	2PX	–	–	−0.1267	–		3PY	–	–	0.1078	–
	2PY	0.1880	0.2489	0.3140	−0.1038		3PZ	0.1259	0.1104	–	0.1445
14(N)	2PZ	0.3280	0.2827	0.1917	0.3685	%Density		3.73	2.97	3.49	4.69
	3PX	–	−0.1039	−0.1336	–						
	3PY	0.1763	0.2323	0.2910	−0.1015		2PZ	–	–	–	0.1022
	3PZ	0.3021	0.2598	–	0.3408	18(C)	3PZ	0.1161	0.1014	–	0.1193
%Density		26.52	27.42	25.40	27.29	%Density		1.35	1.03	–	2.47
	2PX	–	–	0.1079	–		2PY	–	−0.1163	−0.1454	–
	2PY	−0.1601	−0.2137	−0.2704	–	19(C)	2PZ	−0.1971	−0.1758	−0.1428	−0.2140
15(N)	2PZ	−0.2831	−0.2457	−0.1673	−0.3188		3PY	–	−0.1250	−0.1547	–
	3PX	–	–	0.1019	–		3PZ	−0.2111	−0.1872	−0.1518	−0.2259
	3PY	−0.1449	−0.1949	−0.2454		%Density		8.34	9.51	8.85	9.68
	3PZ	−0.2627	−0.2288	−0.1595	−0.2951	21(C)	2PZ	0.1606	0.1461	0.1242	0.1665
%Density		19.58	19.64	20.88	18.87		3PY	–	–	0.1017	–
25(N)	3S	0.1044	0.1005	0.1128	−0.1080		3PZ	0.1862	0.1715	0.1525	0.1876
%Density		1.09	1.01	1.27	1.17	%Density		6.04	5.07	5.91	6.29

forth. The E_{HOMO} is often associated with the capacity of a molecule to donate electrons to an appropriate acceptor with empty molecular orbitals. Also, an increase in the values of E_{HOMO} can facilitate the adsorption and so the inhibition efficiency [14]. The inhibitive properties of compounds depend on the electron densities around the adsorption center and the nucleophilic centers of inhibitor molecules are generally O, N, and/or S atoms. The spatial distribution of electron density for the inhibitor is required to find the probable adsorption center. HOMO atomic orbital coefficients of the studied molecules at B3LYP/6-31G (d,p) level are presented in Table II. As it is seen from the Table II and Figure 2, the HOMO orbitals consist of 61.73–63.04% double bonded S atom (7(S)), and most of the rest are concentrated on the rhodanine group, so the rhodanine fragment will play an important role in bonding of sulfa drugs with metal atom in the corrosion process. The correlation between % densities of 7(S) atom and the %IE for the studied molecules is quite good (0.7824, see Fig. 4).

The E_{LUMO} indicates the ability of the molecule to accept electrons. The lower the value of E_{LUMO}, the most probable it is that the molecule would accept electrons. Consequently, concerning the $E_{HOMO}-E_{LUMO}$ values, lower value of the energy gap difference will cause higher %IE.

The LUMO atomic orbital coefficients of the studied molecules at B3LYP/6-31G(d,p) level are presented in Table III. The LUMO orbital of the studied molecules are concentrated mainly on the azo and benzene sulfonamide groups. Azo group nitrogen (14N and 15N) has the highest LUMO density values in the studied compounds. The 14N atom that is attached to rhodanine group has the highest LUMO density, but we observed no meaningful coefficient of correlation value. However, the 15N atom that is attached to the benzene group of benzene sulfonamide has very high coefficient of correlation value (0.8118) (see Fig. 4). On the other hand, 5(N) atom has the next highest HOMO density value. The 5N atom of the npyrm and ndimepyrm molecules has approximately the same

TABLE IV

Electron affinity, A; Ionization potential, I; absolute electronegativity, χ; absolute hardness, η; and softness, σ values of the studied compounds.

		npyrm	ndimepyrm	ndimetoxpyr	nisox	Fe[a]
HF/ 6-31G(d,p)	A	−0.0392	−0.0408	−0.0382	−0.0353	−0.0408
	I	0.3417	0.3411	0.3423	0.3359	0.2543
	χ	0.1513	0.1502	0.1520	0.1503	0.1068
	η	0.1905	0.1910	0.1903	0.1856	0.1476
	σ	5.2504	5.2367	5.2562	5.3884	6.7771
	A	−0.0333	−0.0349	−0.0326	−0.0392	−0.1856
	I	0.3457	0.3451	0.3462	0.3430	0.2556
HF/6-311G(d,p)	χ	0.1562	0.1551	0.1568	0.1519	0.0350
	η	0.1895	0.1900	0.1894	0.1911	0.2206
	σ	5.2769	5.2627	5.2812	5.2333	4.5336
	A	0.1096	0.1076	0.1087	0.1055	0.1237
B3LYP/6-31G(d,p)	I	0.2348	0.2339	0.2351	0.2327	0.2018
	χ	0.1722	0.1708	0.1719	0.1691	0.1628
	η	0.0626	0.0632	0.0632	0.0636	0.0390
	σ	15.9681	15.8328	15.8290	15.7159	25.6148
	A	0.1170	0.1153	0.1165	0.1096	0.1474
B3LYP/6-311G(d,p)	I	0.2427	0.2419	0.2428	0.2390	0.2039
	χ	0.1798	0.1786	0.1797	0.1743	0.1756
	η	0.0629	0.0633	0.0632	0.0647	0.0283
	σ	15.9109	15.8028	15.8316	15.4631	35.3982

[a] Fe atom values were not used at regression analysis, Units in a.u.

HOMO density values (3.66 and 3.67%). The contribution of HOMO of 5N atom for ndimetoxpyr is determined as 4.72%. In ndimetoxpyr, there are two methoxy groups which makes it different from npyrm and ndimepyrm. In nisox, there is a five-membered isoxazole ring. The effect of the isoxazole ring on the 5N atom is the same as that of npyrm and ndimepyrm molecules, which has the pyrimidine and methyl pyrimidine. Isoxazole ring in nisox makes the contribution of 3C atom decrease. The order of the contribution of 3C atom over HOMO atomic orbitals is presented as follows; nisox < npyrm < ndimepyrm < ndimetoxpyr, and the order is the same as in the values of the experimental corrosion inhibition efficiency (%IE).

The relation between quantum chemical properties and corrosion inhibition is often based on the Lewis theory of acids and bases, and Pearson's hard and soft acids and bases. Chemical potential, μ, and absolute hardness, η, are also two features to characterize any chemical system. The electron affinity, **A;** ionization potential, **I;** absolute electronegativity, **X;** absolute hardness, η; softness, σ values of the studied compounds are presented in Table IV and have been used for correlation in Figure 3. The calculations of the transferred electrons fraction, ΔN of the studied compounds [45–47] was carried out using Eq. (3) and are presented in Table V using a theoretical χ value of 7 eV/mol and η value of 0 eV/mol for iron. The values of ΔN showed inhibi-

TABLE V

ΔN values of the studied compounds.

	npyrm	ndimepyrm	ndimetoxpyr	nisox
HF/6-31G(d,p)	−0.0075	−0.0074	−0.0076	−0.0073
HF/6-311G(d,p)	−0.0249	−0.0247	−0.0250	−0.0241
B3LYP/6-31G(d,p)	−0.0005	−0.0004	−0.0005	−0.0003
B3LYP/6-311G(d,p)	−0.0002	−0.0001	−0.0002	0.0001

TABLE VI

Polarizability (α) and dipole moment, μ (in debye) of the studied compounds using the HF and B3LYP levels.

	HF		B3LYP	
	6-31G(d,p)	6-311G(d,p)	6-31G(d,p)	6-311G(d,p)
		Dipole Moment		
npyrm	5.8917	5.9808	4.9974	5.0895
ndimepyrm	6.0370	6.1232	5.2168	5.2658
ndimetoxpyr	7.1924	7.3341	6.8082	6.9812
nisox	6.8399	7.5408	4.8523	6.4244
		Polarizability		
npyrm	276.273	286.920	318.826	331.462
ndimepyrm	299.177	311.032	344.596	359.040
ndimetoxpyr	304.878	316.001	352.620	325.335
nisox	281.590	280.798	315.777	366.443

tion effect resulting from electrons donation, which agrees with Lukovits et al.'s study [46]. If $\Delta N < 3.6$ (as obtained in this study), the inhibition efficiency increased with increasing electron-donating ability at the metal surface. In this study, the four compounds were the donators of electrons at varying degrees, and the iron surface was the acceptor. The compounds were bound to the metal surface, and thus formed inhibition adsorption layer against corrosion. The best correlation between %IE and ΔN was found at the level HF/6-311G(d,p) (R^2 = 0.8126) (see Fig. 3).

All the calculated values of dipole moment, μ and polarizability, (α) are presented in Table VI. Of all the methods used, no reasonably good correlation was obtained between dipole moment, μ and %IE, but good correlation between %IE and polarizability using HF/6-311G(d,p) (R^2 = 0.8425) was obtained (see Fig. 3).

The Mulliken charges of atoms of the studied molecules are presented in Tables VII. The correlation between %IE and the Mulliken charges were quite good in all the methods used (see Fig. 4). The highest correlation coefficient value of R^2 = 0.8319 was obtained for the 5N atom using the B3LYP/6-31G(d,p) and R^2 = 0.8005 for 6O atom using the B3LYP/6-31G(d,p) level. The 7S atom has highest correlation coefficient of R^2 = 0.8396 using the HF/6-311G(d,p) level. One of the azo nitrogen atoms, 14N has highest correlation coefficient of R^2 = 0.9986 using the HF/6-311G(d,p). The other azo nitrogen atom, 15N also has highest value of R^2 = 0.87 using the HF/6-311G(d,p). The highest value of R^2 = 0.8585 was obtained for the 22S atom using the HF/6-31G(d,p) level. High correlation coefficient values for the 31N heteroatom ranged between 0.9578 and 0.9997(HF/6- 31G(d,p) level.

As seen in Figure 5, ndimetoxpyr has the highest E_{HOMO} and the lowest energy gap (ΔE), and therefore, the order of increasing %IE is similar to that obtained by Abdallah [19] using both weight loss and potentiostatic polarization techniques.

In this investigation, quantitative structure and activity relationship (QSAR) have also been used to correlate the inhibition efficiency of the studied inhibitors and their molecular structure. An attempt to correlate the quantum chemical parameters/descriptors with the average experimental %inhibition efficiencies showed that there was no simple relation or no direct trend relationship can be derived with the inhibition performance of these inhibitors using only one method. The difficulty in obtaining a direct link between quantum chemical parameters/descriptors and %IE serves to emphasize the rather complex interactions that are involved in the corrosion protection afforded by these rather large molecules. Although a number of satisfactory correlations have been reported by other investigators [12, 23, 45, 46] between the inhibition efficiency of various inhibitors used and some quantum chemical parameters, a composite index and a combination of more than one parameter [48–50] has been used to perform QSAR which might affect the inhibition efficiency of the studied molecules. Consequently, a relation may exist between the composite index and the average corrosion inhibition efficiency for a particular inhibitor molecule. Therefore, for this study, parameters have been selected relevant to the activity of the molecules under investigation. The linear model

TABLE VII

Mulliken and Hsummed charges of the studied molecules.

		npyrm		ndimepyrm		ndimetoxpyr		nisox	
	Heteroatom	Mulliken	H Summed	Mulliken	H Summed	Mulliken	H Summed	Mulliken	H Summed
HF/6-31G(d,p)	4(S)	0.3307	0.3307	0.3305	0.3305	0.3308	0.3308	0.3308	0.3308
	5(N)	−0.7522	−0.7522	−0.7522	−0.7522	−0.7522	−0.7522	−0.7594	−0.7594
	6(O)	−0.5195	−0.5195	−0.5196	−0.5196	−0.5198	−0.5198	−0.5357	−0.5357
	7(S)	−0.1567	−0.1567	−0.1575	−0.1575	−0.1559	−0.1559	−0.1511	−0.1511
	14(N)	−0.2029	−0.2029	−0.2034	−0.2034	−0.2037	−0.2037	−0.2072	−0.2072
	15(N)	−0.3013	−0.3013	−0.3014	−0.3014	−0.3009	−0.3009	−0.3070	−0.3070
	22(S)	1.7125	1.7125	1.7119	1.7119	1.7138	1.7138	1.7005	1.7005
	23(O)	−0.6551	−0.6551	−0.6574	−0.6574	−0.6546	−0.6546	−0.6564	−0.6564
	24(O)	−0.6583	−0.6583	−0.6606	−0.6606	−0.6555	−0.6555	−0.6975	−0.6975
	25(N)	−0.8866	−0.5374	−0.8911	−0.5440	−0.8982	−0.5457	−0.9200	−0.5640
	27(N)	−0.6027	−0.6027	−0.6439	−0.6439	−0.6131	−0.6131	−0.2394	−0.2394
	31(N)(31(O)	−0.5778	−0.5778	−0.6186	−0.6186	−0.6520	−0.6520	−0.4955	−0.4955
	32(O)					−0.6530	−0.6530		
	33(O)					−0.6943	−0.6943		
HF/6-311G(d,p)	4(S)	0.2692	0.2692	0.2690	0.2690	0.2692	0.2692	0.2686	0.2685
	5(N)	−0.5858	−0.5858	−0.5858	−0.5858	−0.5858	−0.5858	−0.5855	−0.5855
	6(O)	−0.3959	−0.3959	−0.3959	−0.3959	−0.3962	−0.3962	−0.3961	−0.3961
	7(S)	−0.1118	−0.1118	−0.1126	−0.1126	−0.1111	−0.1111	−0.1162	−0.1162
	14(N)	−0.1469	−0.1469	−0.1473	−0.1473	−0.1479	−0.1479	−0.1457	−0.1457
	15(N)	−0.2545	−0.2545	−0.2546	−0.2546	−0.2542	−0.2542	−0.2569	−0.2569
	22(S)	1.4950	1.4950	1.4915	1.4915	1.4903	1.4903	1.4465	1.4465
	23(O)	−0.6124	−0.6124	−0.6146	−0.6146	−0.6107	−0.6107	−0.6091	−0.6091
	24(O)	−0.6278	−0.6278	−0.6300	−0.6300	−0.6237	−0.6237	−0.6436	−0.6436
	25(N)	−0.6976	−0.4098	−0.7177	−0.4329	−0.7169	−0.4253	−0.7766	−0.4707
	27(N)	−0.4648	−0.4648	−0.5146	−0.5146	−0.4833	−0.4833	−0.2366	−0.2366
	31(N)(31(O)	−0.4467	−0.4467	−0.4966	−0.4966	−0.5081	−0.5081	−0.3158	−0.3158
	32(O)					−0.4602	−0.4602		
	33(O)					−0.5087	−0.5087		
	4(S)	0.2672	0.2672	0.2670	0.2670	0.2666	0.2666	0.2668	0.2668
	5(N)	−0.5075	−0.5075	−0.5076	−0.5076	−0.5071	−0.5071	−0.5080	−0.5080
B3LYP/6-31G(d,p)	6(O)	−0.4392	−0.4392	−0.4393	−0.4393	−0.4393	−0.4393	−0.4392	−0.4392
	7(S)	−0.1271	−0.1271	−0.1283	−0.1283	−0.1267	−0.1267	−0.1303	−0.1303
	14(N)	−0.1665	−0.1665	−0.1670	−0.1670	−0.1675	−0.1675	−0.1675	−0.1675
	15(N)	−0.2827	−0.2827	−0.2832	−0.2832	−0.2812	−0.2812	−0.2838	−0.2838
	22(S)	1.2666	1.2666	1.2632	1.2632	1.2664	1.2664	1.2131	1.2131
	23(O)	−0.5067	−0.5067	−0.5099	−0.5099	−0.5063	−0.5063	−0.5097	−0.5097
	24(O)	−0.5061	−0.5061	−0.5090	−0.5090	−0.5047	−0.5047	−0.5192	−0.5192
	25(N)	−0.6934	−0.3950	−0.6998	−0.4044	−0.7159	−0.4177	−0.6991	−0.4058
	27(N)	−0.4694	−0.4694	−0.5212	−0.5212	−0.4776	−0.4776	−0.1719	−0.1719
	31(N)(31(O)	−0.4343	−0.4343	−0.4844	−0.4844	−0.5126	−0.5126	−0.3590	−0.3590
	32(O)					−0.5080	−0.5080		
	33(O)					−0.5565	−0.5565		
B3LYP/6-311G(d,p)	4(S)	0.2717	0.2717	0.2712	0.2712	0.2712	0.2712	0.2701	0.2701
	5(N)	−0.4063	−0.4063	−0.4057	−0.4057	−0.4056	−0.4056	−0.4060	−0.4061
	6(O)	−0.2881	−0.2881	−0.2880	−0.2880	−0.2881	−0.2881	−0.2882	−0.2883
	7(S)	−0.0534	−0.0534	−0.0546	−0.0546	−0.0529	−0.0529	−0.0589	−0.0589
	14(N)	−0.1146	−0.1146	−0.1141	−0.1141	−0.1142	−0.1142	−0.1141	−0.1141
	15(N)	−0.1976	−0.1976	−0.1988	−0.1988	−0.1979	−0.1980	−0.2002	−0.2002
	22(S)	1.1436	1.1436	1.1385	1.1385	1.1385	1.1385	1.0923	1.0923
	23(O)	−0.4618	−0.4618	−0.4645	−0.4645	−0.4606	−0.4606	−0.4565	−0.4565
	24(O)	−0.4766	−0.4766	−0.4794	−0.4794	−0.4744	−0.4744	−0.5011	−0.5011
	25(N)	−0.5700	−0.3000	−0.5839	−0.3177	−0.5897	−0.3205	−0.6291	−0.3420
	27(N)	−0.3350	−0.3350	−0.3725	−0.3725	−0.3328	−0.3328	−0.2926	−0.1793
	31(N)(31(O)	−0.3110	−0.3110	−0.3476	−0.3476	−0.3677	−0.3677	−0.1919	−0.1920
	32(O)					−0.3507	−0.3507	−0.2266	−0.2266
	33(O)					−0.3883	−0.3884		

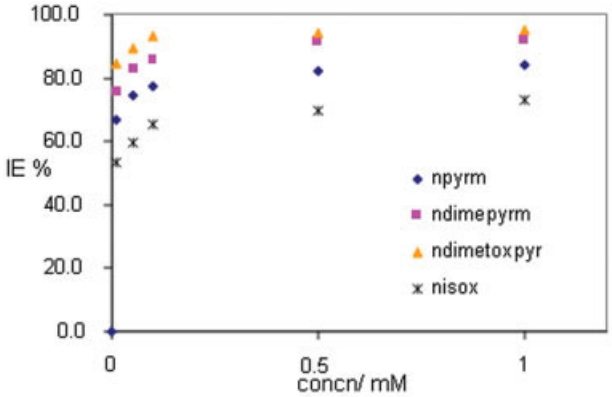

FIGURE 5. Plot of %IE versus inhibitor concentration of the studied molecules. [Color figure can be viewed in the online issue, which is available at www.interscience.wiley.com.]

approximates inhibition efficiency (IE_{cal} %) as in the equation below:

$$IE_{cal} = Ax_jC_i + B \tag{9}$$

where IE_{cal} is the inhibition efficiency, A and B are the regression coefficients determined by regression analysis, x_j is a characteristic quantum index for the inhibitor molecule, and C_i denotes the experiment's concentration of the inhibitor. Such linear approach was not found to be satisfactory for correlating the present results. Consequently, the nonlinear model (NLM) proposed by Lukovits et al. [47] and also used by Khaled et al. [50] for studying the interaction of corrosion inhibitors with metal surfaces in acidic solutions derived from Eq. (10) below based on the Langmuir adsorption isotherm has been employed;

$$IE_i = \frac{(Ax_j + B)C_i}{1 + (Ax_j + B)C_i} \times 100 \tag{10}$$

where IE_i is the inhibition efficiency, A and B are the regression coefficients determined by regression analysis, x_j is a quantum chemical index characteristic for the molecule (j) and C_i denotes the experimental concentration i. However, it was not necessary again in this study to emphasize the type of adsorption because Abdallah [19] had already reported that the compounds obeyed Langmuir adsorption isotherm which goes to support the NLM equation used above which was derived based on the Langmuir adsorption isotherm. In the nonlinear method analysis, multiple regressions were performed on the inhibition efficiencies for the studied compounds and a nonlinear relation of the form below;

$$IE_i = \frac{(6426 \times E_{HOMO} - 1376 \times E_{LUMO} - 1912 \times \mu + 844 \times \alpha - 1963C_i}{1 + (6426 \times E_{HOMO} - 1376 \times E_{LUMO} - 1912 \times \mu + 844 \times \alpha - 1963C_i} \times 100 \tag{11}$$

gave a coefficient of correlation ($R^2 = 0.8998$) between the calculated and experimental efficiencies using the HF/6-311G (d,p) (see Fig. 6). Interestingly, we also like to report that in this studies, the experimental data obtained fits better into the Temkin adsorption isotherm model using the equation below;

$$IE_i = (-93.0E_{HOMO} - 1613E_{LUMO} - 0.1397\mu + 4.570\alpha) + 3.505\ln C_i \tag{12}$$

with a better coefficient of correlation ($R^2 = 0.9825$) between the calculated and experimental efficiencies using the HF/6-311G (d,p) (see Fig. 7).

We can deduce from the relation that the inhibition efficiency is increased by a lower dipole moment (μ) (very little effect from the dipole moment), a significantly higher polarizability (α), an increased (more negative) E_{HOMO} and a decreased (less positive) E_{LUMO}. This demonstrates that a link exist between a composite index of some of the

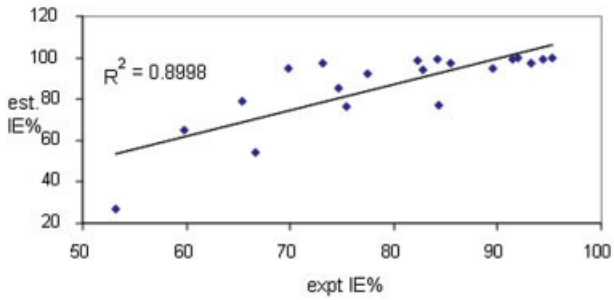

FIGURE 6. Correlation between experimental and calculated/estimated inhibition efficiency of the studied molecules using the Langmuir adsorption isotherm model. [Color figure can be viewed in the online issue, which is available at www.interscience.wiley.com.]

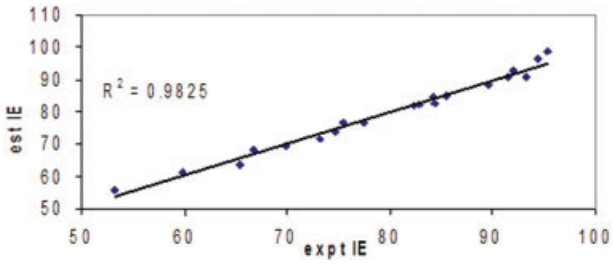

FIGURE 7. Correlation between experimental and calculated/estimated inhibition efficiency of the studied molecules using the Temkin adsorption isotherm model. [Color figure can be viewed in the online issue, which is available at www.interscience.wiley.com.]

quantum chemical parameters and the corrosion inhibition efficiency of the studied molecules. However, it should be pointed out that factors derived from competitive adsorption, the nature of the surface and the solubility may contribute to the establishment of better relationships. Therefore, these results might help in planning of new and effective inhibitor molecules. However, the coefficient of correlation between the experimental and calculated %IE may be improved significantly if a systematic change in the structure of the compounds is considered to avoid overlapping of structural effects.

Conclusions

The rhodanine azo sulfa drugs studied are effective and harmless inhibitors for the corrosion of steel in acidic medium. Our analyses have shown that one quantum chemically-derived parameter is not sufficient in correlating the inhibition activities of these types of molecules. Hence, several parameters or a composite index of more than two or more quantum chemical parameters were taken into consideration to characterize the inhibition activity of the molecules. From this study, we deduced from the QSAR nonlinear relation that the inhibition efficiency is increased by a lower dipole moment (μ), a higher polarizability (α), an increased (less negative) E_{HOMO}, and a decreased (less positive) E_{LUMO}. This QSAR approach is adequately sufficient to forecast the inhibitor effectiveness using the theoretical approach; it may be used to find the optimal group of parameters for predicting a molecule's suitability to be a corrosion inhibitor. Quantum chemical calculations indicated that rhodanine azosulpha drugs that have active centers may form a chemical adsorption layer through the rhodanine molecule, which plays an important role in bonding of the sulfa drugs with the metal atom in the corrosion process. We have reached the conclusion that the synthesis of better corrosion inhibitors can be achieved by controlling all electronic properties and parameters of a selected group of molecules.

References

1. Foad El Sherbini, E. E. Mater Chem Phys 1999, 60, 286.
2. Elayyachy, M.; Hammouti, B.; El Idrissi, A. Appl Surf Sci 2005, 249, 176.
3. Bouklah, M.; Hammouti, B.; Lagrenée, M.; Bentiss, F. Corros Sci 2006, 48, 2831.
4. Ajmal, M.; Mideen, A. S.; Quraishi, M. A. Corros Sci 1994, 36, 79.
5. Fang, J.; Li, J. J Mol Struct (THEOCHEM) 2002, 593, 179.
6. Quraishi, M. A.; Sharma, H. K. Mater Chem Phys 2002, 78, 18.
7. El Sayed, H.; El Ashry, El.; Nemr, A.; Esawy, S. A.; Ragab, S. Electrochim Acta 2006, 51, 3957.
8. Vosta, J.; Eliásek, J. Corros Sci 1971, 11, 223.
9. Zhao, P.; Liang, Q.; Li, Y. Appl Surf Sci 2005, 252, 1596.
10. Yurt, A.; Ulutas, S.; Dal, H. Appl Surf Sci 2006, 253, 919.
11. Xiao-Ci, Y.; Hong, Z.; Ming-Dao, L.; Hong-Xuang, R.; Lu-An, Y. Corros Sci 2000, 42, 645.
12. Wang, D.; Li, S.; Ying, Y.; Wang, M.; Xiao, H.; Chen, Z. Corros Sci 1911, 1999, 41.
13. Bereket, G.; Hür, E.; *Öğ* retir, C. J Mol Struct (THEOCHEM) 2002, 578, 79.
14. *Öğ* retir, C.; Bereket, G. J Mol Struct (THEOCHEM) 1999, 488, 223.
15. Kandemirli, F.; Sagdinc, S. Corros Sci 2007, 49, 2118.
16. Yurt, A.; Bereket, G.; Ogretir, C. J Mol Struct (THEOCHEM) 2005, 725, 215.
17. Ma, H.; Chen, S.; Liu, Z.; Sun, Y. J Mol Struct (THEOCHEM) 2006, 774, 19.
18. Arslan, T.; Kandemirli, F.; Ebenso, E. E.; Love, I.; Alemu, H. Corros Sci 2009, 51, 35.
19. Abdallah, M. Corros Sci 2002, 44, 717.
20. Frisch, M. J.; Trucks, G. W.; Schlegel, H. B.; Scuseria, G. E.; Robb, M. A.; Cheeseman, J. R.; Montgomery, J. A. Jr.; Vreven, T.; Kudin, K. N.; Burant, J. C.; Millam, J. M.; Iyengar, S. S.; Tomasi, J.; Barone, V.; Mennucci, B.; Cossi, M.; Scalmani, G.; Rega, N.; Petersson, G. A.; Nakatsuji, H.; Hada, M.; Ehara, M.; Toyota, K.; Fukuda, R.; Hasegawa, J.; Ishida, M.; Nakajima, T.; Honda, Y.; Kitao, O.; Nakai, H.; Klene, M.; Li, X.; Knox, J. E.; Hratchian, H. P.; Cross, J. B.; Bakken, V.; Adamo, C.; Jaramillo, J.; Gomperts, R.; Stratmann, R. E.; Yazyev, O.; Austin, A. J.; Cammi, R.; Pomelli, C.; Ochterski, J. W.; Ayala, P. Y.; Morokuma, K.; Voth, G. A.; Salvador, P.; Dannenberg, J. J.; Zakrzewski, V. G.; Dapprich, S.; Daniels, A. D.; Strain, M. C.; Farkas, O.; Malick, D. K.; Rabuck, A. D.; Raghavachari, K.; Foresman, J. B.; Ortiz, J. V.; Cui, Q.; Baboul, A. G.;

Clifford, S.; Cioslowski, J.; Stefanov, B. B.; Liu, G.; Liashenko, A.; Piskorz, P.; Komaromi, I.; Martin, R. L.; Fox, D. J.; Keith, T.; Al-Laham, M. A.; Peng, C. Y.; Nanayakkara, A.; Challacombe, M.; Gill, P. M. W.; Johnson, B.; Chen, W.; Wong, M. W.; Gonzalez, C.; Pople, J. A. Gaussian 03, Revision B. 05; Gaussian, Inc.: Wallingford, CT, 2004.

21. Petersson, G. A.; Bennett, A.; Tensfeldt, T. G.; Al-Laham, M. A.; Shirley, W. A.; Mantzaris, J. J Chem Phys 1988, 89, 2193.
22. Becke, A. D. J Chem Phys 1993, 98, 5648.
23. Costa, J. M.; Llush, J. M. Corros Sci 1984, 24, 924.
24. Lee, C.; Yang, W.; Parr, R. G. Phys Rev 1988, B41, 785.
25. Bentiss, F.; Bouanis, M.; Mernari, B.; Traisnel, M.; Vezin, H.; Lagrenee, M. Appl Surf Sci 2007, 253, 3696.
26. Cai, X.; Zhang, Y.; Zhang, X.; Jiang, J. J Mol Struct (THEOCHEM) 2006, 801, 71.
27. Larabi, L.; Benali, O.; Mekelleche, S. M.; Harek, Y. Appl Surf Sci 2006, 253, 1371.
28. Rodriguez-Valdez, L.; Martinez-Villafañe, A.; Glossman-Mitnik, D. J Mol Struct (THEOCHEM) 2005, 716, 61.
29. Rodriguez-Valdez, L.; Martinez-Villafañe, A.; Glossman-Mitnik, D. J Mol Struct (THEOCHEM) 2005, 713, 65.
30. Rodriguez-Valdez, L.; Martinez-Villafañe, A.; Glossman-Mitnik, D. J Mol Struct (THEOCHEM) 2004, 681, 83.
31. Rodriguez-Valdez, L.; Villamisar, W.; Casales, M.; Gonzalez-Rodriguez, J. G.; Martínez-Villafañe, A.; Martínez, L.; Glossman-Mitnik, D. Corros Sci 2006, 48, 4053.
32. Lashkari, M.; Arshadi, M. R. Chem Phys 2004, 299, 131.
33. Sein, L. T., Jr.; Wei, Y.; Jansen, S. A. Comput Theor Polym Sci 2001, 11, 83.
34. Sein, L. T.; Wei, Y.; Jansen, S. A. Synth Met 2004, 143, 1.
35. Blajiev, O.; Hubin, A. Electrochim Acta 2004, 49, 2761.
36. Lebrini, M.; Lagrenee, M.; Vezin, H.; Traisnel, M.; Bentiss, F. Corros Sci 2007, 49, 2254.
37. Gao, G.; Liang, C. Electrochim Acta 2007, 52, 4554.
38. Parr, R. G.; Yang, W. Density Functional Theory of Atoms and Molecules; Oxford University Press: Oxford, UK, 1989.
39. Sen, K. D. Eletronegativity; Structure and Bonding 66; Springer-Verlag: Berlin, 1987.
40. Sen, K. D. Chemical Hardness; Structure and Bonding 80; Springer-Verlag: Berlin, 1993.
41. Parr, R. G.; Yang, W. J Am Chem Soc 1984, 106, 4049.
42. Yang, W.; Parr, R. G. Proc Natl Acad Sci USA 1985, 82, 6723.
43. Parr, R. G.; Donnelly, R. A.; Levy, M.; Palke, W. E. J Chem Phys 1978, 68, 3801.
44. Parr, R. G.; Pearson, R. G. J Am Chem Soc 1983, 105, 7512.
45. Sastri, V. S.; Perumareddi, J. R. Corrosion (NACE) 1997, 53, 617.
46. Lukovits, I.; Kálmán, E.; Zucchi, F. Corrosion (NACE) 2001, 57, 3.
47. Lukovits, I.; Kalman, E.; Palinkas, G. Corrosion (NACE) 1995, 51, 201.
48. Geerlings, P.; De Proft, F. Int J Quantum Chem 2000, 80, 227.
49. Khaled, K. F.; Babic-Samradzija, K.; Hackerman, N. Electrochim Acta 2005, 50, 2515.
50. Khaled, K. F. Appl Surf Sci 2006, 252, 4120.